**J. Cent. South Univ.** (2014) 21: 4553−4562
**DOI:** 10.1007/s11771-014-2460-z

Springer

# 2D registration based on contour matching for partial matching images

ZHANG Jian-wei(张见威), HUANG Da-cheng(黄达承), GUI Jiang-qin(桂姜琴), YE Wen-zhong(叶文忠)

School of Computer Science and Engineering, South China University of Technology, Guangzhou 510006, China



**Abstract:** The mean Hausdorff distance, though highly applicable in image registration, does not work well on partial matching images. An improvement upon traditional Hausdorff-distance-based image registration method is proposed, which consists of the following two aspects. One is to estimate transformation parameters between two images from the distributions of geometric property differences instead of establishing explicit feature correspondences. This procedure is treated as the pre-registration. The other aspect is that mean Hausdorff distance computation is replaced with the analysis of the second difference of generalized Hausdorff distance so as to eliminate the redundant points. Experimental results show that our registration method outperforms the method based on mean Hausdorff distance. The registration errors are noticeably reduced in the partial matching images.

**Key words:** image registration; generalized Hausdorff distance; partial matching image

## 1 Introduction

Image registration is the process of aligning two images of the same scene taken at different time, from different viewpoints, or by different sensors. It geometrically overlays two images, the model image and the floating image, respectively [1]. Having been improved in theory and put into practice successfully, image registration is widely applied in the fields of medicine, remote sensing, computer vision and pattern recognition.

In the medical field, PET/CT-combined instrumentation is a kind of medical imaging equipments based on the image registration technology, which combines PET and CT images respectively captured by different scanners. It can figure out the accurate position diagnosis of lesions, as well as the location before cancer radiotherapy and surgery [2]. In addition, as the functional brain images do not normally convey detailed structural information, they cannot present an anatomically specific localization of functional activity. The multi-image registration technique is thus researched for the purpose of mapping the functional activity into an anatomical image or a brain atlas [3].

Although most medical image registration tasks are 3D non-rigid now, direct 2D-to-2D transformations such as rigid, affine and homographic are often used when sensor metadata or object space information is limited or unavailable. Sometimes, 2D registration would also be used in MRI image fusion by registering a proton density image with its T1 weighted image. Owing to the convenience of their implementation, direct 2D-to-2D registration methods are commonly applied to the commercial software of remote sense image fusion, for example, aligning between synthetic aperture radar (SAR) and optical images. Besides that, infrared sensors are now playing a crucial role in the advance surveillance system as they supply information that a visible sensor cannot provide in a situation of poor lighting, smoke, or fog. An infrared camera is often paired with a visible camera in video surveillance system setups. Hence, 2D registration is needed to find automatically the transformation parameters between two images captured with these two sensors respectively [4]. The other application of 2D registration is to assist multi-focuimage fusion technology. Because of their different focus points, objects in-focus in the first image must be out-focus in the second image, and vice versa. Its mission is to implement the process in which two images with different focus points are fused to produce a new image with extended depth of field [5]. Image registration is one of its important steps.

The intrinsic need of the above applications lies in the registration of images under multi-setting condition toward image fusion. Images of different settings generally have different pixel characteristics since they may come from different kinds of sensors or have different focuses. Therefore, it might be difficult to find the correspondence between pixels from images of the

**Foundation item:** Project(61070090) supported by the National Natural Science Foundation of China; Project(2012J4300030) supported by the Guangzhou Science and Technology Support Key Projects, China
**Received date:** 2013−08−07; **Accepted date:** 2014−05−27
**Corresponding author:** ZHANG Jian-wei, Associate Professor; PhD; Tel: +86−20−39380288−3404; E-mail: jwzhang@scut.edu.cn

same scenes. For instance, in multi-sensor images, contrasts of the images may differ from each other. Even contrast reversal may occur in some regions. As a result, some important features cannot be extracted from both images [6]. That is why many intensity-based methods are not directly available for multi-sensor image registration.

As a common registration measurement, mean Hausdorff distance (MHD) is simple, fast and practical in application to image registration. Hausdorff distance is used to describe the similarity between edge point sets generated from two images. For its computation, every element in set $A$ is matched to its closest element in set $B$ with their closest distance $d$ being computed. The mean Hausdorff distance between $A$ and $B$ is the mean value over all $d$. The MHD-based registration method deals with the edges extracted from images instead of the intensity of pixels. The method is suitable for registration of images under different circumstances. The edges are related to strong gradient response. Even though their gradient magnitudes may be different or irrelevant, corresponding edges exist in both images. MHD's computation is simple and it can also be speeded up by using a distance transform map of the model edge image. It is effective when tackling with a great number of edge points. If edge map can be efficiently extracted, the registration would be robust. Therefore, it has important value in different image registration fields.

Precisely because of noise, perturbation, obstacle, or different image intensity patterns, the edges obtained from images cannot be completely matched. However, due to the existence of redundant edges in the floating edge image，incorrect registration is likely to be obtained. This is because that with a number of redundant edge points, the MHD between those two sets of edge points is large, which will have a negative influence on registration measurement.

In this work, we propose an alignment method that can overcome those limitations. Our objective is to build up a method which should be able to eliminate the redundant edge points in the floating image so as to find accurate transformation parameters. We set about the work through two aspects. Firstly, we use a robust pre-registration method based on the distributions of geometric property difference (DGPD) to avoid the effect of outlier part. Secondly, we propose an approach to remove redundant edge points through the analysis of the second difference of the generalized Hausdorff distance (GHD). After that, the new edge point set of floating image can be aligned using method based on MHD more precisely Experiments have been conducted on simulation images of simple geometric shape, medical images, out-of-focus images and infrared and visible images. The results show that the registration errors of the proposed approach are much lower than those of the original methods based on MHD.

## 2 Related works

Pre-processing of medical images operates before the search for transformational relations, so that the complexity of image registration processing can decrease with fewer disturbances. Edge information pre-processing is one of the pre-processing operations [2]. Edge is an important feature that can reflect structural information. Many researches on image registration used edge information as comparable characteristic. LI et al [7] utilized circular symmetric multi-resolution decomposition to decompose image into low pass subbands and band pass subband. The cross-weighted moments of entire edge information acquired in band pass subband are calculated to obtain rough transformation. The former result is treated as the initial values for the registration at the coarsest level of low pass subbands. The hierarchical registration based on normalized mutual information (NMI) will be implemented from the low resolution level to the high resolution level. TANG et al [8] put forward an approach which used straight lines to fit the edge piecewise by a median method, built an angle difference histogram to realize the coarse matching, and then used mutual information to find out the accurate registration parameters. LU's registration method [9], which extracts the edge feature points using the wavelet multi-scale product, aligns images with a new criterion of edge feature point pair mutual information.

Similarity measurement is an important factor in image registration. HUTTENLOCHER [10] put forward a kind of similarity measurement, Hausdorff distance, imposing registration to binary images (for example, edges of images) with displacement or rotation. It is widely used in researches of different fields. TAN and ZHANG [11] used Hausdorff distance to compute eigenface from edge images for face recognition. GASTALDO and ZUNINO [12] utilized it to research in target detection. A modified Hausdorff distance algorithm was developed by SHAO et al [13], to used for spatial trajectory matching. Generally, the registration method based on it uses MHD as registration measurement. It is defined to describe the similarity between two point sets.

Hausdorff distance between two sets is defined as following.

Given two limited point sets $A=\{a_1, a_2, \cdots, a_p\}$ and $B=\{b_1, b_2, \cdots, b_q\}$, the Hausdorff distance [10] between $A$ and $B$ is

$$d_H(A,B)=\max(h(A,B),h(B,A)) \quad (1)$$

where

$$h(A,B)=\max_{a_i\in A}\min_{b_j\in B}\left\|a_i-b_j\right\| \tag{2}$$

$$h(B,A)=\max_{b_j\in B}\min_{a_i\in A}\left\|b_j-a_i\right\| \tag{3}$$

where ||•|| represents a distance norm between points $a$ and $b$.

Assuming $a$ is a point in point set $A$, the Hausdorff distance from $a$ to point set $B$ is

$$d_{\mathrm{H}}(a,B)=\min_{b\in B}\left\|a-b\right\| \tag{4}$$

The MHD from point sets $A$ to $B$ is

$$\overline{d}_{\mathrm{H}}(A,B)=\frac{1}{S_A}\sum_{a\in A}d_{\mathrm{H}}(a,B) \tag{5}$$

where $S_A$ is the number of points in $A$.

Canny edge operator is used to detect and extract the edge of images. In Refs. [14−15], 3−4 distance transformation is used to represent the distance norm ||•||. Hence, with the method "Chamfer matching" which employs Chamfer distance between boundary points of floating image and those of model image, it is easy to calculate the average value or mean square value as similarity measurement. It can be regarded as a specific practical implementation of the algorithm based on Hausdorff distance. A suitable optimization method can be used to search for the optimum, by using the similarity measurement MHD as the objective function. The parameters corresponding to the minimum are the final registration result.

The registration algorithm based on MHD is effective to rigid registration with two images of high similarity. The transformation from floating image to model image is parameterized by three parameters, rotation angle $\theta$ and two translation parameters $t_x$ and $t_y$, which respectively represent the translation along $x$-direction and $y$-direction of floating image. Assuming that a point's coordinate is ($x$, $y$) in model image, we have ($x'$, $y'$) in floating image corresponding to ($x$, $y$). The transformation equation is described as

$$\begin{bmatrix}x\\y\end{bmatrix}=\begin{bmatrix}\cos\theta & -\sin\theta\\ \sin\theta & \cos\theta\end{bmatrix}\begin{bmatrix}x\\y\end{bmatrix}+\begin{bmatrix}t_x\\t_y\end{bmatrix} \tag{6}$$

NIU et al [16] introduced a method of transformation parameter subspace decomposition on similar transformation and affine transformation, which accelerated calculation speed of Hausdorff distance. Moreover, the method used box distance transformation.

As Hausdorff distance does not consider the overall information of images, it is sensitive to disturbances. WANG et al [17] added an overall factor, difference square between the images to form the difference squared Hausdorff distance and made Hausdorff distance less sensitive to noise. But the difference square Hausdorff distance between each point pair is computationally time-consuming. XIA and LIU [18] solved the 2-D image registration problem by curve matching and alignment starting with a "super-curve". The super-curve is formed by superimposing two related curves in one coordinate system. B-spline fusion technique is used to find a single B-spline approximation of the super-curve and a registration between the two curves simultaneously. Their method can also address the redundant curve problem through matching segments of two curves and finding the partial match between the segmented curves using inflections and cusps.

## 3 Image registration method based on DGPD and GHD

Since the existence of noise, obstacle or difference of imaging circumstances, two imaged under registration may disaccord. If the images being registered are partial matching, the set of redundancy edge points of floating image is the most important negative factor when using MHD as similarity measure. Figure 1 shows the partial matching situation. Figure 1(b) has a redundancy part, compared with the Fig. 1(a) on the left. The ellipse is not present in the model image. As a result, there must be more edge points extracted from Fig. 1(b) than that extracted from image Fig. 1(a). The edge images extracted are shown in Figs. 1(c) and (d), respectively. The redundant edge points are far from the normal edges in the model image. Hence, the mean Hausdorf distance of the set of redundant edge points must be sharply larger than that of real edge points in image. Optimization method will not be able to obtain the optimized result. Table 1 shows the registration results of Fig. 1 using the

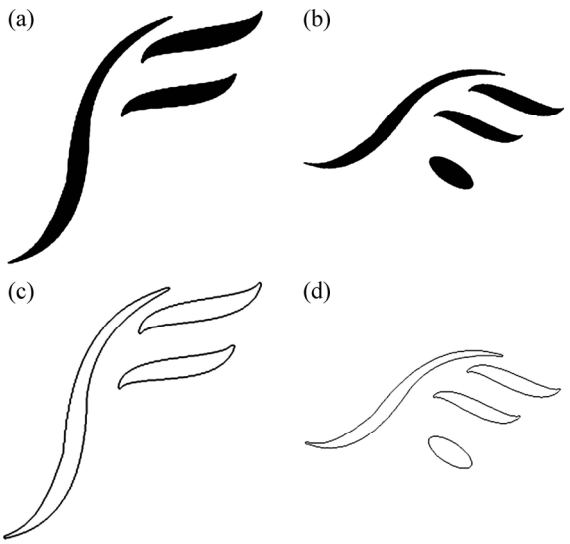


**Fig. 1** Partial matching images and their edge images: (a) Original image; (b) Image with redundancy part; (c) Edge image for (a); (d) Edge image for (b)

**Table 1** Experimental result of MHD method from testing images in Fig. 1 ($\varepsilon$=0.01)

| Transformation parameter | Real value | Experimental result | Absolute error |
|---|---|---|---|
| Rotation angle, $\theta$/(°) | 36 | 32.9733 | 3.0267 |
| Horizontal translation, $t_x$/pixel | 45 | 44.7902 | 0.2098 |
| Vertical translation, $t_y$/pixel | −10 | − 13.2534 | 3.2534 |

registration algorithm based on mean Hausdorff distance. We can see a great error between the experimental result and real value.

Inspired by Refs. [7−8], "coarse to fine" strategy is adopted. To overcome the shortcoming above-mentioned, this work solves the problem through two approaches. One is to lessen the effect of the outlier part; the other is to remove the redundancy edge points. The former one is used as a step of pre-registration, the latter one is the main part of registration with iteration, which makes the result approach to real value step by step. The method proposed in this work is named as "modified generalized Hausdorff distance based method"(MGHD). The overall framework of our registration method can be described as shown in Fig. 2.

### 3.1 Pre-registration based on distributions of geometric property differences

The original MHD method using nonlinear search strategies typically acquires good initial guesses to ensure correct convergence. However, the outlier that doesn't appear in model image prevents it from obtaining accurate result. The geometric properties of image remain relatively stable, i.e., the boundaries between regions, which do not change under illumination changes. The geometric information contained in these image contours is often sufficient to determine the transformation between images [19]. Inspired by Ref. [19], the pre-registration using the key idea of utilization of the geometric properties of image contours is developed. The objective of the step based on distributions of geometric property differences (DGPD) is to lessen the effect of the redundant part. Because of approximate transformation parameters computed by DGPD pre-registration step insensitive to outliers, the next step of redundancy elimination can proceed and final finer registration can get a prefect result.

To describe the method intuitively, a simple illustrative example will be shown in Fig. 3.

Imagine two edge contours shown in Fig. 3 with a rigid transformation. $P$ is an edge point in the model image, while its corresponding point in the floating image is $P'$. The rotation angle between the two images is $\theta$. The slope angles of tangent lines to points $P$ and $P'$ are denoted by $\varphi$ and $\varphi'$, respectively.

The relationship $\theta=\varphi'-\varphi$, is easy to be observed. The relationship exists not only between $P$ and $P'$ but also in every corresponding point pair. So, the rotation angle can be easily recovered from measurements on given point pairs [19]. Obviously, we just compute the geometric measurement difference between every two points respectively from two contours and can find the mode. $\theta$ can be recovered from the mode instead of extracting matching point pairs or establishing explicit feature correspondences. We will represent next that the statistical algorithm is robust in the presence of redundant edge of the floating image.

However, it is not easy to calculate the accurate slope angles of tangent lines, because in general, it is sensitive to noise. Some methods used least squares fitting of a continuous function to fit the edge curve, or used the fitting method in Ref. [8]. But the result generally has some biases, as a result of the difference between discrete curve in digital image and continuous curve in the real world. Consequently, we use gradient orientation of image at the edge points instead of slope angles of the tangent lines. We can observe that the edge detector is also based on gradient variant. Edge is the place that has sharp change in image grayscale. The Canny edge detector uses non-maximum suppression of gradient magnitude to determine the edge points. Gradient orientation is a stable image feature across images. It can be considered as the direction of normal line of the edge point which is perpendicular to its tangent line. In the implementation of the proposed method, Sobel operator is chosen to calculate gradient orientation. Sobel operator is defined as

$$\boldsymbol{G}_X=\begin{bmatrix}-1 & 0 & +1\\ -2 & 0 & +2\\ -1 & 0 & +1\end{bmatrix},\quad \boldsymbol{G}_Y=\begin{bmatrix}+1 & +2 & +1\\ 0 & 0 & 0\\ -1 & -2 & -1\end{bmatrix} \tag{7}$$

where $\boldsymbol{G}_X$ and $\boldsymbol{G}_Y$ can respectively calculate approximate value of difference of grayscale in horizontal and vertical directions by convolving the two windows with an image. Window $\boldsymbol{G}_X$ gives the $X$-component of gradient $\boldsymbol{g}_X$ while $\boldsymbol{G}_Y$ gives the $Y$-component of gradient $\boldsymbol{g}_Y$. Then, the gradient orientation of a point in image can be computed by

$$\theta=\arctan\left(\frac{\boldsymbol{g}_Y}{\boldsymbol{g}_X}\right) \tag{8}$$

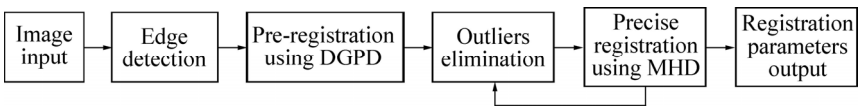


**Fig. 2** Flowchart of overall framework of MGHD method

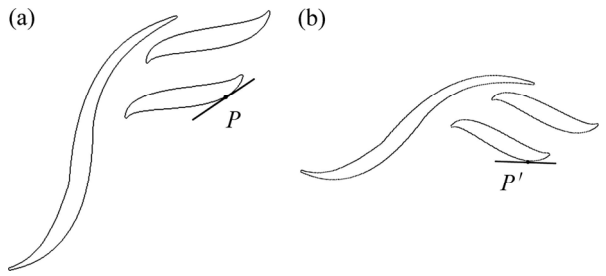


**Fig. 3** Contour (a) and its rotated version (b) (Tangent lines at corresponding points $P$ and $P'$ on two curves are indicated)

With respect to the edge point sets $C_M$ and $C_F$ from model image $M$ and floating image $F$, we use Sobel operator to calculate the gradient orientation at each edge point in the two images. Assuming that $\varphi(u)$ is the gradient orientation at edge point $u$ and the range of $\varphi(u)$ is [0, 359], while $p_i \in C_M$, $q_j \in C_F$, thereinto, $i$=1, 2, ⋯, $N_M$, $j$=1, 2, ⋯, $N_F$, $N_M$ and $N_F$ are the numbers of edge points of $C_M$ and $C_F$, respectively, the difference between the gradient orientations of $p_i$ and $q_j$ can be represented as $\theta(i, j)=\varphi(q_j)-\varphi(p_i)$. After rounded off, $\theta(i, j)$ varies from 0° to 359°. They are binned into $n$ orientation bins to build a angle histogram of $\theta(i, j)$. The peak value of the histogram can be considered as the approximate rotation angle between two images. This is because that the difference of gradient orientations of each corresponding point pair, $\theta(k,l)$, must be approximate to rotation angle between two images, and converge on the neighborhood of it. On the contrary, the difference of gradient orientations of non-corresponding point pair will vary from 0° from 359° randomly. With regard to the redundancy edge points in floating image, analogously, the gradient orientation differences between them and the edge points in model image are also random and will be thrown into different bins uniformly. In this case, gradient orientation differences of non-corresponding point pairs will not affect the peak value's location. Actually, the histogram of the gradient orientation difference is equivalent to the cross-correlation between the two distributions of edge gradient orientations. The meaning behind finding the peak value in histogram is to maximize the cross-correlation between the two distributions under a specific shift. In other words, using the method, the optimal estimate of a transformation parameter is actually obtained by maximizing the similarity of two distributions of geometric property. As shown in Fig. 4,

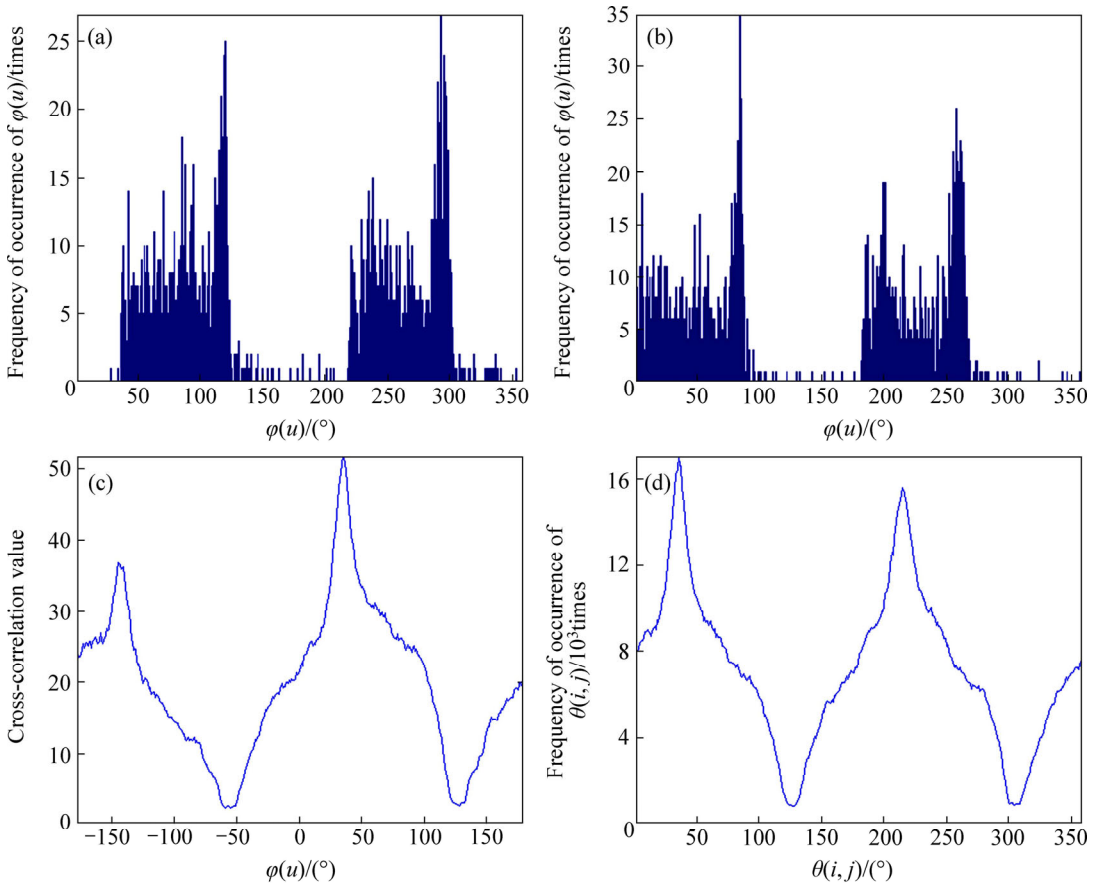


**Fig. 4** Distribution of gradient orientations, gradient orientations difference and cross-correlation between two distributions of gradient orientations: (a) Distribution of gradient orientations generated from Fig. 3(a); (b) Distribution of gradient orientations generated from Fig. 3(b); (c) Cross-correlation sequence between distribution of edge gradient orientations (a) and (b); (d) Distribution of gradient orientations difference generated from Figs. 3(a) and (b)

the distribution of gradient orientation difference generated from two contours in Fig. 3 looks similar to the cross-correlation sequence from their original distributions of edge gradient orientations. They convey the same information of transformation parameter with the peak. Figure 4(c) shows the cross-correlation sequence over the lag range [−179°, 179°]. In that case, the two distributions in Figs. 4(a) and (b) are seen as two jointly stationary random processes. It is notable that there are two crests in the distribution of gradient orientations difference. It is just because that each component of the object in Fig. 3 is approximately centrosymmetric. Each of them has a high similarity with its rotated version of 180°. After rotation of 180°, the distribution of gradient orientations of edge points is similar to that of original image. But the second crest is always not as high as peak which represents true rotation angle.

Having compensated for the rotation between the images, we can calculate horizontal direction translation $t_X$ and vertical direction translation $t_Y$ between the two images using the same fashion [19]. $x(u)$ is assumed to be horizontal coordinate at edge point $u$. After the rotation angle of floating image is adapted, for horizontal coordinate of $p_i$ and $q_j$, their difference values of each other are computed, which can be represented as $X(i, j)$= $x(q_j)-x(p_i)$. A histogram of $X(i, j)$ is built in the same way in order to get the peak value as the estimated translation $t_X$. As the same, the translation $t_Y$ can be got using the method. Those histograms of $\theta(i, j)$ or $X(i, j)$ are named as distributions of geometric property differences (DGPD).

Up to now, we build up a pre-registration method based on DGPD. The method does not have to extract correspondences of point pairs, but can convert the observability of parameters through point pairs to the observability through distributions of geometric property difference. In conclusion, the method using statistical histogram of geometric property is insensitive to the redundancy edge. It is because the geometric property differences between non-corresponding point pairs tend to distribute randomly and they will be thrown into different bins uniformly. Hence, the effect of the redundancy edge points can be weakened by the major normal edge points through the subtraction. From another perspective, it is possible that since the most part of floating contour can find their matching part, the method can still have sufficient coincident contour points to compute correct geometric properties. Hence, the distribution of geometric properties of floating edge is not significantly disturbed; the transformation parameters can still be recovered from the histogram of geometric properties difference.

Looking back to Fig. 1, there is a redundant oval in float image, but the approximate transformation parameters can be extracted using DGPD method. The histogram of gradient orientation difference shown in Fig. 5 is nearly the same as the version without outliers shown in Fig. 4(d). In the distribution, the evident highest peak can be located as rotation angle. As listed in Table 2, from histogram of the geometric properties, the estimated transformation is close to the real value. The absolute errors are smaller than the registration result shown in Table 1.

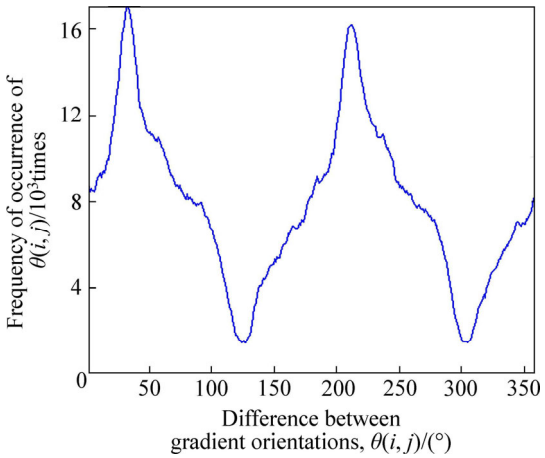


**Fig. 5** Distribution of gradient orientation difference generated from two contours in Fig. 1

**Table 2** Result of pre-registration based on DGPD from testing images in Fig. 1

| Transformation parameter | Actual value | Experimental result | Absolute error |
|---|---|---|---|
| Rotation angle, $\theta$/(°) | 36 | −35 | 1 |
| Horizontal translation, $t_x$/pixel | 45 | 45 | 0 |
| Vertical translation, $t_y$/pixel | −10 | −11 | 1 |

### 3.2 Eliminating redundant edges based on generalized Hausdorff distance

Huttenlocher put forward the notion of partial Hausdorff distance [20] which is an extension of Hausdorff distance. It is also named generalized Hausdorff distance (GHD), which is used in automatic moving object extraction [21].

With respect to given point sets $A$ and $B$, the conception of GHD is described in mathematics expression as

$$h_k(A,B) = \underset{a\in A}{kth}\ \min_{b\in B}\|a-b\| \tag{9}$$

$$h_l(B,A) = \underset{b\in B}{lth}\ \min_{a\in A}\|b-a\| \tag{10}$$

where $kth$ denotes the $k$-th ranked in a set of values, $l$th denotes the $l$-th ranked in a set of values Equation (9) is named as forward partial Hausdorff distance and Eq. (10) is the reverse distance. GHD can describe a subset of

whole point set. That character makes GHD more flexible than MHD. With respect to each point $a$ in point set $A$, its distance with the nearest point in point set $B$ is calculated. Consequently, a sequence of distance value can be obtained, and the selected $k$-th minimum value is denoted by $h_k(A, B)$. If $h_k(A, B)$ is equal to $d$, we can say that there are at least $k$ points in point set $A$, from which the distance to the nearest points in $B$ is less than $d$. If $k$ in Eq. (9) is equal to the number of points in $A$, the equation degrades into the equation of Hausdorff distance. Compared with Hausdorff distance, GHD can reflect the relationship between two point sets in the round.

The proposed method uses the second order difference sequence of GHD to analyze the distance between two point sets so as to eliminate the unwanted points. The edge point set of the model image is denoted by $C_M$ and that of the floating image is denoted by $C_F$, which contains redundancy edge called as $C_{FE}$ and real edge as $C_{FR}$ corresponding to $C_{MR}$ in $C_M$. The inaccurate result obtained through MHD method is due to that $C_F$ is not totally corresponding to $C_M$. When $C_{FE}\neq\varnothing$, it will greatly affect the registration result. After pre-registration, $C_{MR}$ and $C_{FR}$ are roughly registered, but the outlier edge points $C_{FE}$ are overall far from $C_M$. So, GHD $h_k(C_{FE}, C_M)$ must be larger than $h_k(C_{FR}, C_M)$ generally and become larger and larger with the increment of $k$. The first order difference gives the variation of GHD, while the second order difference gives the variation of the former. The maximum of second difference demonstrates the point with rapid change. The point can be considered as demarcation point between $C_{FR}$ and $C_{FE}$. So, it is possible to analyze the second order difference of GHD and eliminate the outliers [22]. The analysis and eliminating procedure is described below. After sorting GHD $h_k(C_F, C_M)$ by $k$ ascendingly, the obtained distance sequence is denoted by $H_k(C_F, C_M)$. The proposed method calculates second order difference of $H_k(C_F, C_M)$ by $k$, as

$$\Delta^2 H_k(C_F, C_M) = \Delta H_{k+d}(C_F, C_M) - \Delta H_{k-d}(C_F, C_M) \quad (11)$$

where

$$\Delta H_k(C_F, C_M) = H_{k+d}(C_F, C_M) - H_{k-d}(C_F, C_M) \quad (12)$$

And $d$ is natural number. Then, the maximum of $\Delta^2 H_k(C_F, C_M)$ is computed and its index is marked as $k_{max}$. In the distance sequence $H_k(C_F, C_M)$, the GHD value increases slowly before the position of $k_{max}$, while it soars after the position of $k_{max}$. So, in the sequence $H_k(C_F, C_M)$, the values, whose index satisfies $k \geq k_{max}$, describe the distance of edge points far from $C_M$. Accordingly, those points can be considered as redundant points and be eliminated from $C_F$. If there are a lot of redundant edge points in $C_{FE}$ or the they are near to $C_{FR}$, an evident maximum of second order difference of the sequence $H_k(C_F, C_M)$ may not be obtained. At this moment, we can compute the average value of $H_k(C_F, C_M)$ and its variance $\sigma_H^2$, then choose values in the sequence $H_k(C_F, C_M)$ satisfying $(H_k(C_F, C_M) - \overline{H_k}(C_F, C_M))^2 > \lambda \times \sigma_H^2$. The chosen values describe the distance of edge points far from $C_M$. Those points can be deleted as well. Real number greater than 1 can be chosen as the value of $\lambda$.

Let's recall the two contours shown in Fig. 1. After adjusting floating image with transformation parameters got from pre-registration, the sequence $H_k(C_F, C_M)$ and its second order difference $\Delta^2 H_k(C_F, C_M)$ can be computed. They are plotted in a curve graph in Fig. 6. An evident inflection point in $H_k(C_F, C_M)$'s curve in Fig. 6 (a) with the index of 28 can be sent. It can be regarded as the demarcation point between $C_{FR}$ and $C_{FE}$. We also can see a maximal second order difference in $\Delta^2 H_k(C_F, C_M)$'s

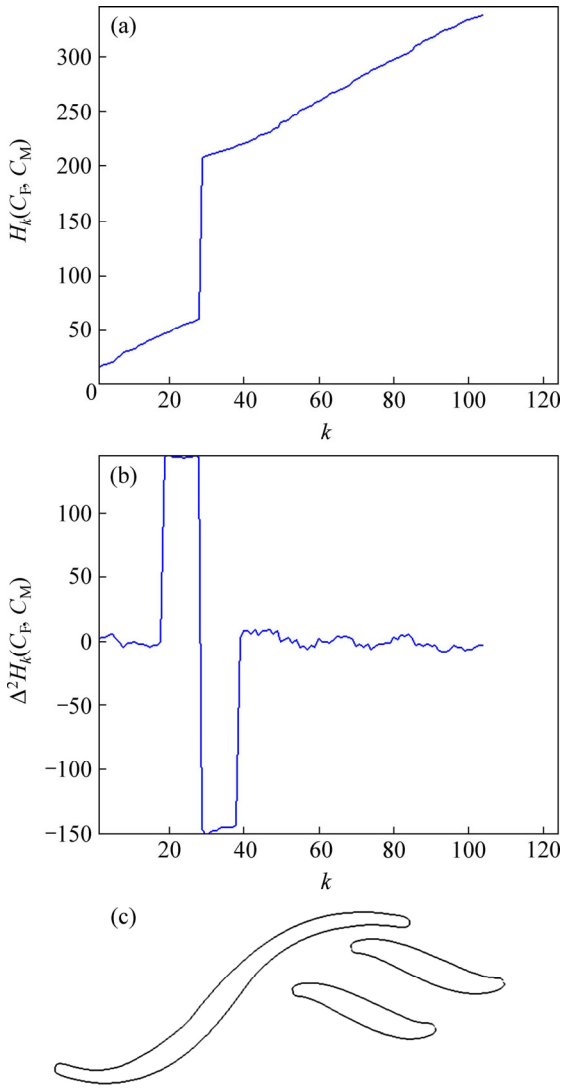


**Fig. 6** Visualization of analysis of GHD and its result of redundancy elimination: (a) Curve of GHD sequence from registration process of two images in Fig. 1; (b) Curve of second difference of GHD from registration process of two images in Fig. 1; (c) Edge of floating image after redundant edge elimination

curve in Fig. 6(b) with the index of 28. The distance values after the index 28 in sequence $H_k(C_F, C_M)$ describe the points far from $C_M$. So, the outlier points can be eliminated to get a new floating edge image shown in Fig. 6(c) through above analysis.

After the elimination of the redundant edge points, we can have a finer registration step to find more precise registration parameters. The new point sets $C_F$ and $C_M$ can be applied in ordinary MHD method with an optimization algorithm which helps to search the optimized result. If a specific accuracy is not arrived, the above steps of outliers elimination and finer registration can be repeated until MHD $\overline{d}_H(C_F, C_M)$ is smaller than a given constant or the point number of $C_F$ is less than a given constant.

Based on the method mentioned above, with the elimination of outlier points, accurate transformation parameters can be obtained after several iterations. Because the transformation parameters obtained by pre-registration is approximate to the real value, the optimization method can have a good initial guess. Hence, it searches in a local domain near the optimal value and converges to optimal value rapidly and exactly instead of searching global solution space.

## 4 Experiments and results

To verify the accuracy and effectiveness of the MGHD method, simulation experiments are carried out with different kinds of images. Comparisons are made not only with usual method based on Hausdorff distance but also with mutual-information-based method. Registration experiment is made with a pair of medical images about hand. The floating image has two objects interlaced together. With respect to the images shown in Fig. 7(a) is the model image, Fig. 7(b) shows the floating image with an additional shadow part because of some imaging problems. There is a rigid transformation relationship between them. The transformation parameters between them are (−35°, 38, −50) where −35° is the rotation angle (negative sign means the rotation is anticlockwise); 38 and −50 pixels are translation parameters in horizontal direction and vertical direction, respectively. The comparable experimental results are listed in Table 3. And the registered image and the difference between the model image and the registered image are shown in Figs. 7(c) and (d),

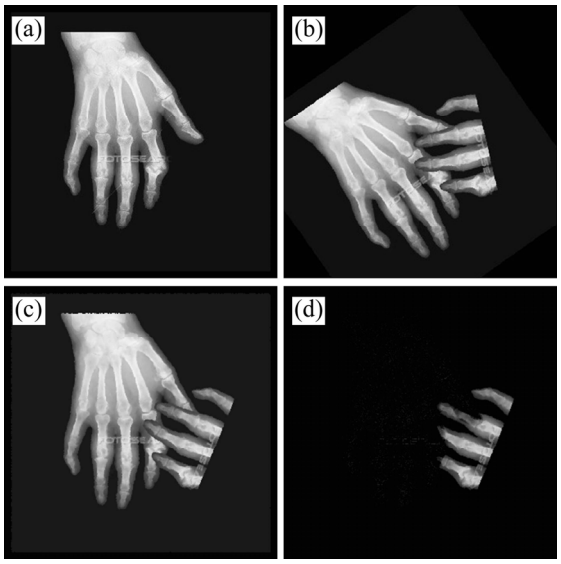


**Fig. 7** Medical images about hands: (a) Model image (b) Floating image with an additional object; (c) Registered image; (d) Difference between (a) and (c)

respectively. $\varepsilon$ shown in the header of tables below represents the condition of termination in the optimization algorithm, which controls the accuracy of parameters acquired.

Let's consider another abnormal situation shown in Fig. 8, whose model image has an obstructed part. The results of our MGHD method and comparison with the result of other algorithms are listed in Table 4. Because of the obstruction for many other reasons, the edge extracted from model image will lack a segment of edge. As a consequence, the non-matching parts in the edge of floating image can be considered as outlier or redundancy. They will corrupt the registration result. As listed in Table 4, the registration result of usual MHD method shows greater errors. The proposed method can eliminate the anomalous parts and have a more accurate registration result.

Another experiment is implemented on a pair of out-of-focus images shown in Figs. 9 (a) and (b). Non-ideal focusing may be caused by aberrations of the imaging optics. The images are both partially in focus, and partially out of focus in varying degrees. Their out-of-focus regions are different. The edge images extracted from them may be diverse. There must be some non-correspondence edges between two images. Table 5 shows comparable experiment result of usual method

**Table 3** Experimental result of MGHD from testing images in Fig. 7($\varepsilon$=0.01)

| Transformation parameter | Real value | Method based on MHD | MI method | Pre-registration based on DGPD | MGHD method |
|---|---|---|---|---|---|
| Rotation angle, $\theta$/(°) | −35 | −42.5988 | −20.0000 | −31 | −34.9841 |
| Horizontal translation, $t_x$/pixel | 38 | 51.7335 | 20.0000 | 45 | 38.1532 |
| Vertical translation, $t_y$/pixel | −50 | −13.8092 | −6.6412 | −43 | −50.0849 |

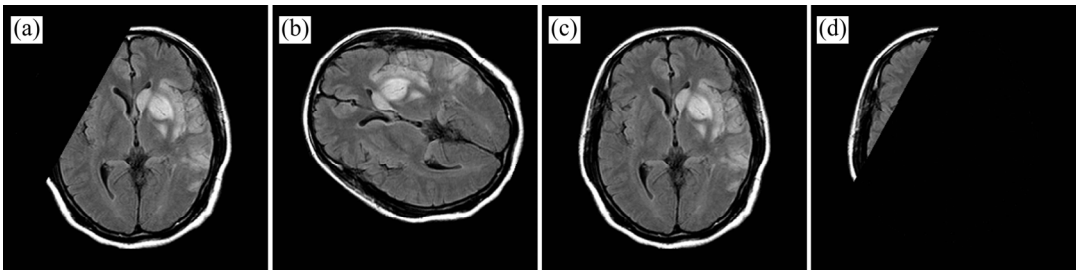


**Fig. 8** Situation with obstructed part in model image: (a) Model image with deficiency part; (b) Intact floating image; (c) Registered image; (d) Difference between (a) and (c)

**Table 4** Experimental result of testing images in Fig. 8 ($\varepsilon$=0.01)

| Transformation parameter | Real value | Method based on MHD | MI method | Pre-registration based on DGPD | MGHD method |
|---|---|---|---|---|---|
| Rotation angle, $\theta$/(°) | −68 | −83.7659 | −20.0000 | −73 | 67.9857 |
| Horizontal translation, $t_x$/pixel | 11 | 1.8144 | 16.2439 | 17 | 10.7157 |
| Vertical translation, $t_y$/pixel | 78 | 46.1779 | 3.2604 | 74 | −78.0614 |

**Table 5**: Experimental result of testing images (Figs. 9(a) and (b))

| Transformation parameter | Real value | Method based on MHD | MI method | Pre-registration based on DGPD | MGHD method |
|---|---|---|---|---|---|
| Rotation angle, $\theta$/(°) | 12.5° | 20.0205 ° | 12.6317 ° | 8 ° | 12.5208 ° |
| Horizontal translation, $t_x$/pixel | 1 | 9.7694 | 0.2331 | 4 | 0.4825 |
| Vertical translation, $t_y$/pixel | 2 | 0.0103 | 1.2436 | 1 | 1.3179 |

**Table 6**: Experimental result of testing images (c) and (d) in Fig. 9 (ε=0.01)

| Transformation parameter | Real value | Method based on MHD | MI method | Pre-registration based on DGPD | MGHD method |
|---|---|---|---|---|---|
| Rotation angle, $\theta$/(°) | −32 | −30.4554 | −32.2888 | −28 | −32.0425 |
| Horizontal ranslation, $t_x$/pixel | 8 | 9.1667 | 12.9720 | 7 | 8.0934 |
| Vertical translation, $t_y$/pixel | −9 | −8.7380 | 0.8856 | −9 | −8.6092 |

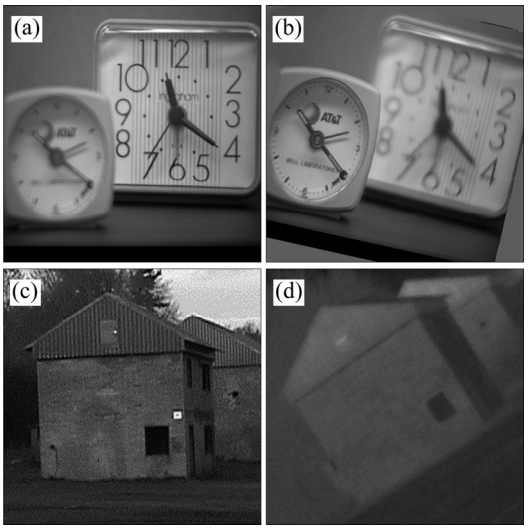


**Fig. 9** Two registration experiments: out-of-focus images and infrared and visible images: (a) Model out-of-focus image; (b) Floating out-of-focus image; (c) Visible model image; (d) Infrared floating image

based on MHD and the proposed method.

We also test our method on infrared image and visible image shown in Fig. 9(c) is the visible model image, while Fig. 9(d) is the infrared floating image. As they are obtained from different sensors, non-correspondence edges must exist.

The experiments show that the mutual-information-based method is not suitable for the situation in Figs. 7 and 8. Besides, we can conclude that MGHD method is superior to the usual method based on MHD in partial matching images.

## 5 Conclusions

1) Estimating transformation parameter by using the distributions of geometric properties as a prepared registration without extracting characteristic points and establishing point correspondences is insensitive to redundant edge.

2) Eliminating the redundant edge points through the analysis of second order difference of GHD can release the effect of the redundant edge points.

3) Pre-registration result is approximate to the real value, which makes the optimization method just search a local domain near the evaluated values rather than global solution space, improving accuracy and searching

speed.

4) It should also be noted that much future work should be done to improve the MGHD method. We simply use Canny edge detector to extract edge; but if an image has a lot of textures, complicated or fragmental edge will be extracted. Imposing MGHD method on too many edge points will cost much computational time. On the contrary, contours just like a single regular circle will lead to the invalidation of our pre-registration method. If the shapes of contours extracted from multi-sensor images seem quite different, the pre-registration step may not be able to get good initial parameters. Hence, to extract suitable edge for MGHD is an important factor. The method is designed and tested for 2D rigid registration, and moreover, many real-world problems are 3D, deformable registration involving different subjects. Therefore, the proposed works can be treated as the first version of our trial. Further work will be done to take other transformation models into consideration and to build up a general component to deal with partial matching situation.

## References


[1] ZITOVA B, FLUSSER J. Image registration methods: A survey [J]. Image and Vision Computing, 2003, 21(11): 977−1000.

[2] HAN Fang-fang, YANG Jin-zhu, LIU Yang. Research on preprocessing algorithm for PET-CT image registration [C]// Proceedings of Int Conf on Optoelectronics and Image Processing. Haiko, China: ICOIP, 2010: 266−269.

[3] GHOLIPOUR A, KEHTARNAVAZ N, BRIGGS R, DEVOUS M, GOPINATH K. Brain functional localization: A survey of image registration techniques [J]. IEEE Trans Medical Imaging, 2007, 26(4): 427−451.

[4] BILODEAU G A, TORABI A, MORIN F. Visible and infrared image registration using trajectories and composite foreground images [J]. Image and Vision Computing, 2011, 29(1): 41−50.

[5] WANG Zhao-bin, MA Yi-de, GU Jason. Multi-focus image fusion using PCNN [J]. Pattern Recognition, 2010, 43(6): 2003−2016.

[6] KIM Y S, LEE J H, RA J B. Multi-sensor image registration based on intensity and edge orientation information [J]. Pattern Recognition, 2008, 41(11): 3356−3365.

[7] LI Hui, PENG Yu-hua, LI Deng-wang, XU Jian-hua. A new multiresolution medical image registration algorithm based on intensity and edge information [C]// Proceedings of 4th Int Conf on Natural Computation. Jinan, China: ICNC, 2008: 13−17.

[8] TANG Jin-hua, YANG Xin, LIU Chunyan, WU Xiu-qing. Image registration based on fitted straight lines of edges [C]// Proceedings of 6th World Congress on Intelligent Control and Automation. Dalian, China: ICA, 2006: 9782−9785.

[9] LU G, YAN J, KOU Y, ZHANG J. Image registration based on criteria of feature point pair mutual information [J]. IET Image Processing, 2011, 5(6): 560−566.

[10] HUTTENLOCHER D P, KLANDERMAN G A, RUCKLIDGE W J. Comparing images using the Hausdorff distance under translation [C]// Proceedings of IEEE Computer Society Conf on Computer Vision and Pattern Recognition. Champaign, USA: IEEE, 1992: 654−656.

[11] TAN Hua-chun, ZHANG Yu-jin. Computing Eigenface from edge images for face recognition based on Hausdorff distance [C]// Proceedings of 4th Int Conf on Image and Graphics. Chengdu, China: ICIG, 2007: 639−644.

[12] GASTALDO P, ZUNINO P. Hausdorff distance for target detection [C]// IEEE International Symposium on Circuits and Systems. Scottsdale, USA: IEEE, 2002: 661−664.

[13] SHAO Fei, CAI Song-mei, GU Jun-zheng. A modified Hausdorff distance based algorithm for 2-dimensional spatial trajectory matching [C]// Proceedings of 5th Int. Conf. on Computer Science and Education. Heifei, China: ICCSE, 2010: 166−172.

[14] BORGEFORS G. Hierarchical chamfer matching: A parametric edge matching algorithm [J]. IEEE Trans. on Pattern Analysis and Machine Intelligence, 1988, 10(6): 849−865.

[15] BARROW H G, TENENBAUM J M, BOLLES R C, WOLF H C. Parametric correspondence and chamfer matching: Two new techniques for image matching [C]// Proceedings of 5th Int Joint Conf on Artificial Intelligence. Cambridge, Massachusetts: JCAZ, 1977: 659−663.

[16] NIU Li-pi, JIANG Xiu-hua, ZHANG Wen-hui, SHI Dong-xin. Image registration based on Hausdorff distance [C]// Proceedings of Int Conf on Networking and Information Technology. Manila, Philippines: ICNIT, 2010: 252−256.

[17] WANG A, SUN Xi-yan, ZHOU Xiao-xing. Difference squared Hausdorff distance based medical image registration [C]// Proceedings of Control and Decision Conference, Guiyang, China: CSC, 2011: 4270−4272.

[18] XIA Ming-hui, LIU Bede. Image registration by “Super-Curves” [J]. IEEE Trans on Image Processing, 2004, 13(5): 720−732.

[19] GOVINDU V, SHEKHAR C. Alignment using distributions of local geometric properties [J]. IEEE Trans on Pattern Analysis and Machine Intelligence, 1999, 21(10): 1031−1043.

[20] HUTTENLOCHER D P, KLANDERMAN G A, RUCKLIDGE W J. Comparing images using the Hausdorff distance [J]. IEEE Trans on Pattern Analysis and Machine Intelligence, 1993, 15(9): 850−863

[21] XU Hai-feng, YOUNIS A A. Automatic moving object extraction for content-based applications [J]. IEEE Trans on Circuits and Systems for Video Technology, 2004, 14(6): 796−812.

[22] ZHANG Jian-wei, HAN Guo-qiang, WO Yan. Image registration based on generalized and mean Hausdorff distances [C]// Proceedings of Int Conf on Machine Learning and Cybernetics. Guangzhou, China: ICMLC, 2005: 5117−5121.


**(Edited by DENG Lü-xiang)**